This document is downloaded from DR-NTU (https://dr.ntu.edu.sg)
Nanyang Technological University, Singapore.

Coaxial Ag–Base Metal Nanowire Networks with High Electrochemical Stability for Transparent and Stretchable Asymmetric Supercapacitors

Park, Sangbaek; Tan, Alvin Wei Ming; Wang, Jiangxin; Lee, Pooi See

2017

Park, S., Tan, A. W. M., Wang, J., & Lee, P. S. (2017). Coaxial Ag–base metal nanowire networks with high electrochemical stability for transparent and stretchable asymmetric supercapacitors. Nanoscale Horizons, 2(4), 199-204.

https://hdl.handle.net/10356/83008

https://doi.org/10.1039/c7nh00024c

© 2017 The Royal Society of Chemistry. This is the author created version of a work that has been peer reviewed and accepted for publication by Nanoscale Horizons, The Royal Society of Chemistry. It incorporates referee’s comments but changes resulting from the publishing process, such as copyediting, structural formatting, may not be reflected in this document. The published version is available at: [http://dx.doi.org/10.1039/c7nh00024c].

Downloaded on 13 Sep 2024 13:09:27 SGT

Please do not adjust margins

View Article Online
DOI: 10.1039/C7NH00024C

Journal Name

COMMUNICATION

Coaxial Ag–Base Metal Nanowire Networks with High Electrochemical Stability for Transparent and Stretchable Asymmetric Supercapacitors

Received 00th January 20xx,
Accepted 00th January 20xx

DOI: 10.1039/x0xx00000x

www.rsc.org/

Sangbaek Park,[a] Alvin Wei Ming Tan,[a] Jiangxin Wang[a] and Pooi See Lee*[a]

Transparent and stretchable Ag–Ni and Ag–Fe core–shell nanowire networks were fabricated as a cathode and anode, respectively, for asymmetric supercapacitors. Both electrodes showed reversible stretchability up to 100% strain and exhibited high electrochemical stability and specific capacitances of ~ 3 mF cm^{-2} with 50% optical transmittance. The asymmetric device assembled with PVA/KOH electrolyte demonstrated high operating voltage of 1.6 V and excellent capacitance retention (92%) over 5000 cycles even after stretching to 35% strain.

A critical need in wearable electronic systems is to find suitable energy storage units that offer similar physical or optical properties as the wearable electronics and provide integration capability while maintaining their electrochemical functions under deformation[1]. Supercapacitors have been widely studied as a possible candidate to meet such requirements with advantages of high power density, long cycling stability, low cost, safe operation and simple configuration[2,3]. Pioneering studies based on carbon nanomaterials including carbon nanotubes and graphene have demonstrated various types of supercapacitors: stretchable[4, 5], transparent[6, 7], stretchable & transparent[8, 9], asymmetric stretchable[10, 11], asymmetric transparent[12] devices. However, these carbon nanomaterials–based supercapacitors mostly exhibit extrinsic stretchability depending on the strain applied to the substrate before material deposition, which retards the integration with other electronics[13].

Metal nanowire networks embedded in a polymer matrix are one of the most competitive stretchable electrodes with several advantages, including good mechanical robustness and higher conductivity and transparency than carbon nanotube or graphene[14]. Considering that most carbon materials usually need pre-straining of polymer substrates to secure enough stretchability, the intrinsic stretchability of nanowire network structure makes them an ideal fit in the integrated systems[15-17]. Recently, diverse applications with both stretchable and transparent properties have been reported by using silver nanowires (Ag NWs), e.g. sensors[18], heaters[19], light-emitting diodes[20], electroluminescent devices[21]. In contrast, despite its versatile structural characteristics, Ag NW has been constrained by its oxidation issue in its application in electrochemical energy storage devices. Ag atoms on the surface of Ag NW can be electrochemically oxidized or rapidly dissolved when exposed to the electrolyte containing particular ions (S^{2-}, Cl^-, Br^-, I^-, OH^-, H^+) in the typical potential range used to charge electrochemical cells[22]. In the case of supercapacitors, up to date, Ag NWs have been just used as a supporter to provide the one-dimensional nanostructure[23-25] or as an auxiliary conductor to deposit other stable conductor[26] or tested only at the lower potential window than 0 V vs. NHE[27]. Our preliminary work demonstrated the stretchable Ag–Zn batteries where embedding Ag NWs into the polymer matrix allowed only the exposed part of Ag NWs to be oxidized and the embedded part to maintain its conductivity, although very thick Ag NWs layer was necessary[28]. Therefore, despite the attractive potential of Ag NWs as stretchable and transparent metal nanowire networks, enhancing the electrochemical stability of Ag NWs is the fundamental challenge which holds the key to the progress of electrochemical energy storage devices.

Having a protective coating could help to provide solution to prevent Ag NWs against corrosion[29]. Several studies have focused on the formation of noble metals (Au, Pt, Pd) or their alloy sheath on Ag NWs through the galvanic replacement reaction[30, 31]. Recently, Lee et al reported 5 nm thick-Au coated Ag NWs as a stretchable and transparent electrode and applied to a symmetric sandwich-type supercapacitor[32]. The electrode showed enhanced air stability during 4 weeks after gold coating, but peak currents of cyclic voltammetry curves were rapidly degraded to 2 % of its original value after only 50 cycles with 45 wt.% loss of Ag NWs. It indicates that the electrochemical oxidation affects the rapid degradation rather than the air oxidation. Some have been interested in nickel

[a] School of Materials Science and Engineering, Nanyang Technological University Singapore, 50 Nanyang Avenue, Singapore 639798. Email: pslee@ntu.edu.sg

† Electronic Supplementary Information (ESI) available: Transmission spectra, SEM, EDS line-scanning, CV, stability test, stretchability test, demonstration and experimental details. See DOI: 10.1039/x0xx00000x

This journal is © The Royal Society of Chemistry 20xx

Please do not adjust margins

Published on 19 April 2017. Downloaded on 20/04/2017 08:52:05.

Nanoscale Horizons Accepted Manuscript

View Article Online
DOI: 10.1039/C7NH00024C

Published on 19 April 2017. Downloaded on 20/04/2017 08:52:05.

coating instead of gold and reported 20 nm-thick Ni coated Cu NWs[33] and 55 nm-thick Ni coated Ag NWs[34] as air stable and transparent electrodes although those are not stretchable. Metal oxides (TiO_2, Al:ZnO, F:SnO_2) on Ag NWs have been also attempted by vacuum deposition and showed high air stability over 2 months, but exhibited poor bending durability due to their brittle natures[35-37]. Hence, further breakthroughs are necessary to achieve an ideal nanowires-based electrode with stretchable, transparent and electrochemically stable characteristics.

Here we propose for the first time that coaxial Ag–base metal core-shell nanowire networks could be electrochemically stable in alkaline aqueous electrolyte over broad potential range. In this structure, base metal shell provides a physical barrier, as well as cathodic protection that the oxidation of Ag NW core is suppressed by the sacrificial oxidation (or corrosion), because the base metal shell is more reactive than Ag. Moreover, a native oxide/hydroxide layer formed on the surface of base metal shell can be fully utilized for the surface Faradaic redox reactions, leading to high specific capacitance. To prove this concept, Ag–Ni and Ag–Fe core-shell nanowire networks were fabricated and transferred into a polyurethane acrylate matrix. As a result, both electrodes exhibited highly conductive, stretchable and transparent properties, as well as high electrochemical stability in KOH electrolyte. Furthermore, a 1.6 V asymmetric full cell supercapacitor, assembled using Ag–Ni NWs as a positive electrode and Ag–Fe NWs as a negative electrode, exhibits energy density as high as 0.68 mWh cm^{-3} (superior to reported flexible/stretchable symmetric devices based on transparent carbon nanomaterial electrodes[35, 36]), high power density (313 mW cm^{-3}) as well as good cycling stability (5000 times with 92% capacitance retention) and stretchability (91% capacitance retention with 35% strain).

In order to obtain highly conductive and electrochemically stable core-shell nanowire networks, we employed the sequential deposition method instead of conventional approach. The previous methodology for the coating of protective layer on Ag NWs are categorized into two types: (i) metal shells were formed on each Ag NWs through solution process and then the core-shell nanowires were infiltrated with elastomer[32, 33]; (ii) Ag NWs were transferred into the elastomeric substrate and then metal shells were coated onto the surface of Ag NW networks[34]. Former case allows all sides of the Ag NW to be covered with protective layer, but it increases the junction resistance between two core-shell nanowires especially when easily oxidized metal is used as the shell layer. Conversely, the latter case secures the high conductivity of the Ag NW networks, but the Ag NWs were only partially covered with protective layer, leading to the exposed Ag region when deforming the substrate (discussed in more detail later). Unlike traditional methods, herein, Ag NWs were deposited and thermally sintered on the glass substrate first, and then Ag NW networks were directly covered with thin and dense Ni or Fe nanoshells thoroughly by electrodeposition before transferred into a polyurethane acrylate (PUA) polymer matrix (see the Experimental section

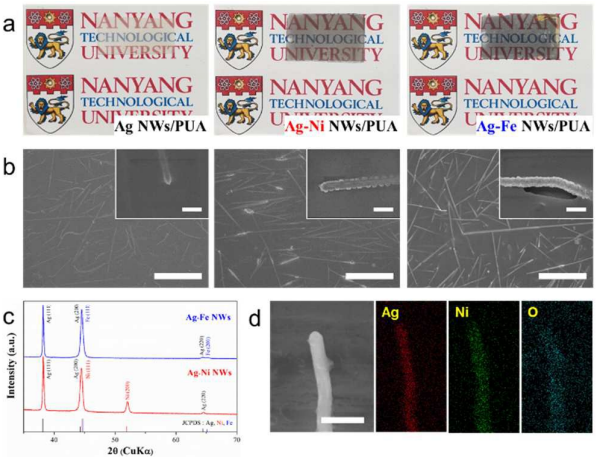

Fig. 1 Visual transparency, surface, crystal structure and elemental analysis of Ag NWs and Ag–metal NWs electrodes. (a) Photographs and (b) SEM images of Ag NWs (left), Ag–Ni NWs (middle) and Ag–Fe NWs (right) embedded in PUA substrates. Scare bar: 10 μm (inset: 500 nm). (c) XRD graphs of Ag–Ni NWs and Ag–Fe NWs. (d) EDS elemental mapping of a Ag–Ni NW, indicating nickel oxides on the surface.

for details, ESI†). It allows the resultant conductive and stretchable Ag NW networks to be bodily encapsulated in the metal nanoshells, which is advantageous to the protection of Ag NWs from corrosion.

Fig. 1a shows typical examples of the Ag NWs, Ag–Ni NWs and Ag–Fe NWs embedded in PUA substrates; the electrodes are optically transparent (%T at 550 nm = 78.7%, 54% and 51.2%, respectively; Fig. S1, ESI†) with high conductivity (sheet resistance: 3.1, 1.2 and 2.9 Ω sq^{-1}, respectively). The color change from yellow (Ag) to gray (Ni) or dark blue (Fe) is attributed to the change in absorption properties by the shell layer coating. Top-view scanning electron microscopy (SEM) images of electrodes showed that the Ag NWs are thoroughly covered with 20 nm-thick Ni and Fe nanoshells and those core-shell nanowires are inlaid into the surface layer of the PUA polymer (Fig. 1b). It is noted that the percolation network of Ag NWs is well-preserved even after Ni and Fe coating, which is a key to maintain high transmission value by retaining substantial unblocked area in the whole electrode. To confirm the crystal structure of core-shell nanowires, the X-ray diffraction (XRD) was carried out (Fig. 1c). Ag–Ni NWs and Ag–Fe NWs electrodes display the standard diffraction peaks which are well indexed to Ag metal (JCPDS card No. 04-0783), and the diffraction peaks of indicative of Ni metal (JCPDS card No. 04-0850) and Fe metal (JCPDS card No. 06-0696) are also found, respectively. Energy dispersive spectroscopy (EDS) elemental mapping of Ag–Ni NWs exhibits that Ni element is uniformly distributed throughout the nanowire while Ag element has a narrower distribution at the core region of the nanowire (Fig. 1d). Also, line-scan profile of Ni presents a double-hump pattern with a relative low content in the center, while that of Ag exhibits one broad peak in the central region (Fig. S2), which illustrates the core-shell structure. Interestingly, O element is also detected all over the nanowire, implying that native oxide layer was successfully formed on the surface of Ni nanoshells during post-annealing of Ag–Ni NWs.

Nanoscale Horizons Accepted Manuscript

This journal is © The Royal Society of Chemistry 20xx

Please do not adjust margins
View Article Online
DOI: 10.1039/C7NH00024C

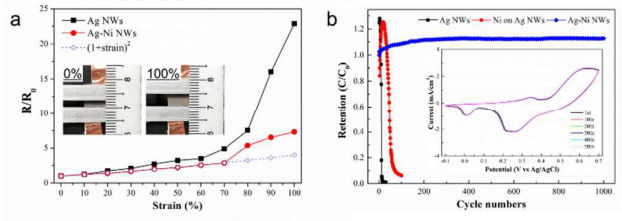

Fig. 2 Stretchability and electrochemical stability characterization of electrodes. (a) The relative changes in resistance of Ag NWs and Ag–Ni NWs embedded PUA substrates under progressively increasing strains. Inset shows photographs of a Ag–Ni NWs/PUA electrode at 0% and 100% strain. (b) Percentage capacitance retention in aqueous 1 M KOH electrolyte of Ag–Ni NWs/PUA in comparison with those of Ag NWs/PUA and Ni coated Ag NWs/PUA. The as-measured CV curves of Ag–Ni NWs along with cycles are presented in the inset. (The CV curves of Ag NWs/PUA and Ni coated Ag NWs/PUA are presented in Fig. S2, ESI†)

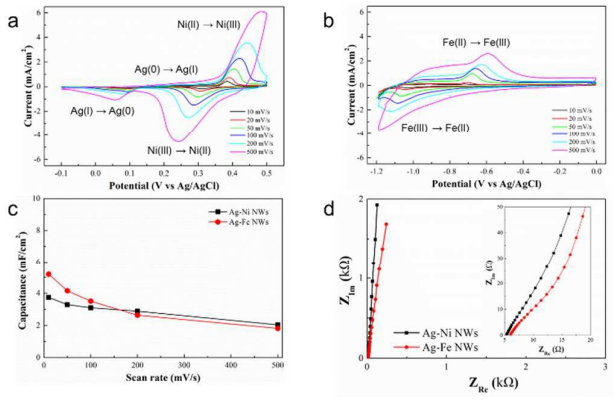

Fig. 3 Electrochemical characterization of Ag–metal NWs embedded PUA. CV curves of (a) a Ag–Ni NWs electrode and (b) a Ag–Fe NWs electrode as a cathode and an anode for supercapacitor, respectively, at various scan rates from 10 mV s^{-1} to 500 mV s^{-1} in a 1 M KOH electrolyte with a three-electrode system. (c) Specific capacitance of the Ag–Ni and Ag–Fe NWs electrode as a function of the scan rates. (d) Nyquist plots of Ag–Ni and Ag–Fe NWs electrode under same conditions. The inset shows the high frequency region.

To test the stretchability, the electrical resistance changes of the Ag NWs and Ag–Ni NWs electrodes were measured with increasing strain up to 100% (Fig. 2a and its inset). The resistance of the bare Ag NWs increases steadily at relatively small strains and rises steeply after increasing strain up to 70%, which is good agreement with the previous reported work[20]. The relative changes in resistance of Ag–Ni NWs show a similar tendency, but its increment is much smaller than that of Ag NWs. Enhanced stretchability is attributed to the reinforced connection between each nanowire by Ni deposition. As mentioned above, the sheet resistance of Ag NWs was dramatically decreased from 3.1 to 1.2 Ω sq^{-1} after Ni coating. It means that Ni nanoshells improve the junction conductance between nanowires, leading to the overall electrode conductivity improvement[31]. Also, the resistance changes of Ag–Ni NWs are well-matched with the ideal resistance curve, $R/R_0 = (1 + strain)^2$, implying that there is no loss of nanowire interconnections up to 70% strain[40]. It reveals that tightly covered Ni nanoshells contribute to preventing the break-up of the Ag NW networks during stretching.

The electrochemical stability of Ag–Ni NWs/PUA was evaluated in comparison with the conventional Ag NWs/PUA and Ni coated on Ag NWs/PUA (used as control sample). A three-electrode system was used with Pt counter and Ag/AgCl reference electrode in the KOH aqueous electrolyte. Fig. 2b shows the percentage capacitance retention of three electrodes calculated from cyclic voltammetry (CV) curves. Remarkably, Ag–Ni NWs exhibit superior electrochemical stability than other electrodes and gave 112% capacitance retention after 1000 cycles. There is no significant change in the CV curve of Ag–Ni NWs, whereas rapid current drops are observed in CV curves of other electrodes within the initial 50 cycles (Inset of Fig. 2b and Fig. S3, ESI†). Outstanding electrochemical stability is attributed to the unique coaxial Ag–Ni nanowire networks which provide (i) the impermeable Ni barrier covering Ag NW networks thoroughly and (ii) galvanic protection that Ag NWs is cathodically protected by the sacrificial corrosion of nickel. In the case of Ni coated on Ag NWs/polymer prepared by the previous method, only the exposed area from the polymer matrix can be covered by Ni shells because electrodeposition of Ni was conducted after transfer of Ag NWs into polymer[34]. While Ni redox reaction is the main reaction in our Ag–Ni NWs, the control samples (the Ni coated Ag NWs/polymer after transfer) is plagued by the Ag redox reaction (Fig. S2), inducing the oxidation of Ag core-nanowire and the loss of conductivity. Although electrochemical stability can be enhanced by increasing the thickness of Ni coating on the control sample, the Ag redox reaction was present even in the 550 nm-thick Ni coated Ag NWs/PUA (from the CV curves); accordingly, it lost 94% of its original capacitance during 100 cycles (Fig. S4, ESI†). It signifies that an impermeable barrier which covers the Ag NWs thoroughly is important to protect the Ag NWs from corrosion. Meanwhile, in the case of the previous reported Au coated Ag NWs, although each Ag NW was densely covered with Au layer through solution method, the peak current in CV curves rapidly dropped to 2%[32]. The authors interpreted that the core Ag NWs are partially exposed to electrolyte due to defects or pores in the Au surface. As Au is more stable than Ag, such exposed region cannot be protected at all. It means that galvanic protection plays an important role for enhancing the electrochemical stability of Ag–Ni NWs.

The electrochemical properties of the Ag–Ni and Ag–Fe NWs electrodes were systematically studied. Fig. 3a and b show the CV curves of the Ag–Ni and Ag–Fe NWs electrodes at the different scan rates from 10 mV s^{-1} to 500 mV s^{-1}, respectively. The peak current of the CV curves increases linearly with the square root of the scan rate for both Ag–Ni and Ag–Fe NWs electrodes (Fig. S5, ESI†), indicating that the surface faradaic reactions are diffusion-controlled and thus the charge-transfer reactions at electrode/electrolyte interface are relatively fast[38]. The Ag–Ni NWs electrode exhibits two pairs of redox peaks in the CV curve at 5 mV s^{-1}, where the sharp and intense peaks at 0.38 and 0.31 V is related to the redox reactions of Ni(II) ↔ Ni(III)[42] and the broad and small peaks at 0.24 and 0.12 V is related to the redox reactions of Ag(0) ↔ Ag(I)[43] as follows:

Published on 19 April 2017. Downloaded on 20/04/2017 08:52:05.
Nanoscale Horizons Accepted Manuscript

Please do not adjust margins

View Article Online
DOI: 10.1039/C7NH00024C

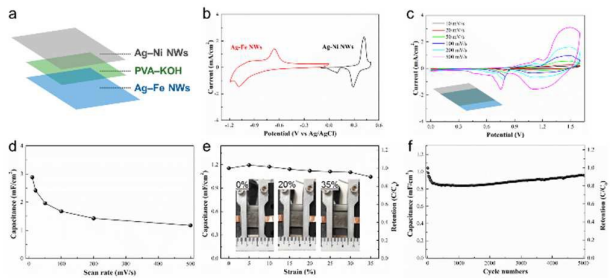

Fig. 4 Device characterization of an asymmetric supercapacitor. (a) Scheme for the fabrication of a sandwich-type supercapacitor based on Ag–Ni and Ag–Fe NWs with PVA–KOH gel electrolyte. (b) Comparison of CV curves of Ag-Ni NWs and Ag-Fe NWs at a scan rate of 100 mV s^{-1} in 1 M KOH aqueous solution. (c) CV curves of the device at various scan rates in the PVA–KOH gel electrolyte. (d) Specific capacitance of the device as a function of the scan rates. (e) Change of the specific capacitance of the device with increasing strain. Inset shows photographs of the device at various strains. (f) Cycling performance of the device after stretching to 35% strain.

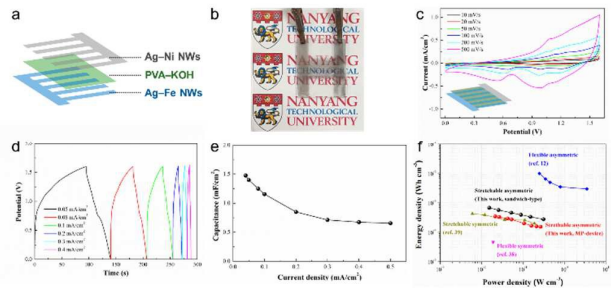

Figure 5. Device characterization of a micro-patterned supercapacitor. (a) Schematic illustration for the fabrication of a micro-patterned (MP) supercapacitor based on Ag–Ni and Ag–Fe NWs with PVA–KOH gel electrolyte. (b) Photograph of the transparent MP supercapacitor, of which transparency is demonstrated by the visibility of the NTU University logo below. (c) CV curves of the MP device at various scan rates. (d) Galvanostatic charging–discharging curves of the MP device at various current densities. (e) Specific capacitance of the MP device as a function of current density. (f) Ragone plot of the sandwich-type and micro-patterned asymmetric supercapacitors. The volumetric energy and power density of the devices are compared with those of other flexible or stretchable transparent supercapacitors[12, 38, 39].

$$NiO + OH^- \leftrightarrow NiOOH + H_2O + e^-$$

$$2Ag + 2OH^- \leftrightarrow Ag_2O + H_2O + 2e^-$$

It is noteworthy that the Ag redox reaction in the Ag–Ni NWs electrode is reversible and maintained over 1000 cycles as shown in Fig. 2b. Typically, the surface oxidation increases the junction resistance between Ag NWs, leading to the loss of conductivity. In the Ag–Ni NWs, however, only a small part of Ag NWs is exposed to the electrolyte through the defects of the Ni layer[32], where Ag could be reversibly oxidized and reduced without the loss of conductivity of the electrode. Actually, Ag–Ni NWs electrode maintained its morphology and conductive properties even after 1000 cycles (Fig. S6a, ESI†). In contrast, when the Ni electrodeposition duration was reduced from 25 s to 15 s, the main peak of CV curves was Ag redox reaction (Fig. S7) because Ag nanowires only partially covered with Ni shells. It indicates that Ni layer should be thick enough to cover the Ag NWs thoroughly and fully protect the Ag NWs from corrosion. Meanwhile, the Ag–Fe NWs electrode exhibits a pair of redox peaks at −0.72 and −1.03 V in the CV curve at 5 mV s^{-1}, which corresponded to the redox reaction of Fe(II) ↔ Fe(III)[41]. Similar to Ag–Ni NWs, the morphology and conductivity of Ag–Fe NWs electrode also maintained after 1000 cycles (Fig. S6b, ESI†). The areal capacitance of the Ag–Ni NWs and Ag–Fe NWs is estimated to be 3.8 mF cm^{-2} and 5.2 mF cm^{-2} at a scan rate of 10 mV s^{-1}, decreasing to 2.0 and 1.8 mF cm^{-2} with increasing the scan rate to 500 mV s^{-1}, presenting 54% and 35% capacitance retention, respectively (Fig. 3c). These specific capacitances and rate capabilities are much higher than those of transparent carbon nanomaterials-based electrodes[38, 39] as well as NWs/polymer composites EDLC electrodes[32, 44]. Both electrodes have almost vertical trends in the low-frequency region of the Nyquist plots (Fig. 3d), which is representative of an ideal capacitive performance[13]. Moreover, the indistinct appearance of semicircles in the high-frequency region suggests a very low charge transfer resistance at electrode/electrolyte interface[45], which is consistent with excellent rate capabilities.

To evaluate the Ag–base metal NWs electrodes for device applications, the Ag–Ni NWs and Ag–Fe NWs were sandwiched around a PVA/KOH gel electrolyte to assemble an asymmetric supercapacitor as illustrated in Fig. 4a. The potential windows of both electrodes at the same scan rate presents the maximum operation potential of the device can reach up to 1.7 V. As shown in Fig. 4c, the CV curves of Ag–Ni NWs//Ag–Fe NWs device exhibit the redox humps, attributed to the contribution from the faradaic reactions of electrodes. The CV curve is well-maintained even at high scan rates up to 500 mV s^{-1}, suggesting a good rate capability of the asymmetric cell. The specific capacitance value of the device obtained at 500 mV s^{-1} is 1.2 mF cm^{-2}, retaining 41% of the initial value (2.9 mF cm^{-2}) at a scan rate of 10 mV s^{-1} (Fig. 4d). Moreover, the asymmetric cell shows good stretchability that the capacitance could be maintained at 91% with the increasing strain to 35% (Fig. 4e and Fig. S8). The slightly increased capacitances by 3.5% and 1.6% when stretched to 5% and 10%, respectively, is attributed to the improved contact between electrode/electrolyte interface by the shearing force during stretching[46]. Furthermore, even after stretching to 35% strain, 92% of its initial capacitance is retained for 5000 cycles, demonstrating a good long-term stability of the device (Fig. 4f). The sharply decrease in the initial 200 cycles is related to the irreversible Fe/Fe(II) reaction[47] and gradually increases with increasing cycle likely due to an activation process[48]. These results demonstrate the pioneering concept of stretchable asymmetric supercapacitor based on transparent Ag NWs electrodes for the first time.

To emphasize the versatile application potential of the Ag–base metal NWs electrodes, the micro-patterned (MP) device was designed as a prototype for the transparent and stretchable asymmetric supercapacitor (Fig. 5a). The NTU logos behind the device could be seen clearly, exhibiting transparent feature of the device (Fig. 5b). A CV response of the MP device in the potential range of 0–1.6 V exhibits a broader redox peak in comparison with that of the sandwich-type (Fig. 4c and Fig.

Published on 19 April 2017. Downloaded on 20/04/2017 08:52:05.
Nanoscale Horizons Accepted Manuscript

This journal is © The Royal Society of Chemistry 20xx

Please do not adjust margins
View Article Online
DOI: 10.1039/C7NH00024C

Published on 19 April 2017. Downloaded on 20/04/2017 08:52:05.

5c) because the capacitances of the positive (Ag–Ni NWs) and negative (Ag–Fe NWs) electrodes were modulated to balance the charges. Galvanostatic charge/discharge curves of the transparent MP device were obtained at various current densities in the range from 0.05 to 0.5 mA cm^{-2} (Fig. 5d). Potential plateaus were observed in the charge and discharge curves, confirming the contribution of the faradaic reaction, which is in good agreement with the CV tests. The MP device exhibits the specific capacitances of 1.48 mF cm^{-2} at 0.05 mA cm^{-2} and a high capacitance retention rate of 45% up to 0.5 mA cm^{-2} (Fig. 5e). These capacitance values are almost half of those in the sandwich-type device, because each MP electrodes only cover 50% of full area in the MP device. The MP device also exhibits good stretchability, where the original capacitance could be maintained up to 20% strain (Fig. S9). Additionally, the two devices that were connected in series successfully lighted up a LED while maintaining the transparent nature (Fig. S10). To our best knowledge, this is the first demonstration of the transparent and stretchable asymmetric supercapacitor. The sandwich-type and micro-patterned asymmetric supercapacitors can deliver a maximum energy density of 0.68 and 0.35 mWh cm^{-3} and still maintain 0.28 and 0.16 mWh cm^{-3} at a high power density of 313 and 267 mW cm^{-3}, respectively (Fig. 5f). These values are much higher than those of the transparent symmetric supercapacitors based on nanoengineered carbon films[38] or microstructure graphene membrane[39].

Conclusions

In summary, Ag–Ni and Ag–Fe core–shell nanowire networks embedded in polyurethane acrylate polymer substrates have been successfully fabricated as a new family of transparent and stretchable conducting electrodes for supercapacitors through a facile electrodeposition and transfer method. The unique structure where the welded Ag nanowire network is thoroughly covered with Ni or Fe nanoshells guarantees high electrochemical stability of the electrodes in KOH electrolyte over the typical operating potential window, as well as providing high specific capacitances (~ 3 mF cm^{-2} with 50% optical transmittance) by surface faradaic reactions of metal oxide/hydroxide layers. The Ag–Ni $NWs_{(+)}$//Ag–Fe $NWs_{(-)}$ asymmetric supercapacitor operated at 1.6 V delivers high energy density (0.68 mWh cm^{-3}), high power density (313 mW cm^{-3}), and excellent cycling stability (5000 cycles, 92% retention) with good stretchability (35% strain, 91% retention). Furthermore, a transparent and stretchable asymmetric supercapacitor is demonstrated for the first time by combining the micro-patterned Ag–base metal NWs electrodes. This work offers a possible route toward electrochemically durable metal nanowire transparent conductors, which is versatile for developing advanced electrochemical devices in integrated wearable electronic systems.

Acknowledgements

This research is funded by the NRF Competitive Research Programme NRF-CRP13-2014-02, that is supported by the National Research Foundation, Prime Minister's Office, Singapore. The authors thank G. Cai in the EDS line measurements.

Notes and references

1 W. Liu, M. S. Song, B. Kong and Y. Cui, *Adv. Mater.*, 2017, **29**, 1-34.
2 B. C. Kim, J.-Y. Hong, G. G. Wallace and H. S. Park, *Adv. Energ. Mater.*, 2015, **5**, 1500959.
3 W. Du, R. Liu, Y. Jiang, Q. Lu, Y. Fan and F. Gao, *J. Power Sour.*, 2013, **227**, 101-105.
4 C. Yu, C. Masarapu, J. Rong, B. Wei and H. Jiang, *Adv. Mater.*, 2009, **21**, 4793-4797.
5 J. Zang, C. Cao, Y. Feng, J. Liu and X. Zhao, *Sci. Rep.*, 2014, **4**, 6492.
6 K. Lee, H. Lee, Y. Shin, Y. Yoon, D. Kim and H. Lee, *Nano Energ.*, 2016, **26**, 746-754.
7 P. Kanninen, N. D. Luong, H. Sinh le, I. V. Anoshkin, A. Tsapenko, J. Seppala, A. G. Nasibulin and T. Kallio, *Nanotechnology*, 2016, **27**, 235403.
8 T. Chen, H. Peng, M. Durstock and L. Dai, *Sci. Rep.*, 2014, **4**, 3612.
9 P. Xu, J. Kang, J.-B. Choi, J. Suhr, J. Yu, F. Li, J.-H. Byun, B.-S. Kim and T.-W. Chou, *ACS Nano*, 2014, **8**, 9437-9445.
10 Q. Tang, M. Chen, C. Yang, W. Wang, H. Bao and G. Wang, *ACS Appl. Mater. Interfaces*, 2015, **7**, 15303-15313.
11 Q. Tang, W. Wang and G. Wang, *ACS Appl. Mater. Interfaces*, 2016, **8**, 27701–27709.
12 N. Li, C. Zhi and H. Zhang, *Electrochim. Acta*, 2016, **220**, 618-627.
13 J. Pu, X. Wang, R. Xu and K. Komvopoulos, *ACS Nano*, 2016, **10**, 9306–9315.
14 T. Sannicolo, M. Lagrange, A. Cabos, C. Celle, J. P. Simonato and D. Bellet, *Small*, 2016, **12**, 6052-6075.
15 C. Yan, J. Wang, X. Wang, W. Kang, M. Cui, C. Y. Foo and P. S. Lee, *Adv. Mater.*, 2014, **26**, 943-950.
16 Z. Luo, Y. Jiang, B. D. Myers, D. Isheim, J. Wu, J. F. Zimmerman, Z. Wang, Q. Li, Y. Wang, X. Chen, V. P. Dravid, D. N. Seidman and B. Tian, *Science*, 2015, **348**, 1451-1455.
17 B. Tian, P. Xie, T. J. Kempa, D. C. Bell and C. M. Lieber, *Nat. Nanotech.*, 2009, **4**, 824-829.
18 W. Hu, X. Niu, R. Zhao and Q. Pei, *Appl. Phys. Lett.*, 2013, **102**, 083303.
19 S. Hong, H. Lee, J. Lee, J. Kwon, S. Han, Y. D. Suh, H. Cho, J. Shin, J. Yeo and S. H. Ko, *Adv. Mater.*, 2015, **27**, 4744-4751.
20 J. Liang, L. Li, X. Niu, Z. Yu and Q. Pei, *Nature Photon.*, 2013, **7**, 817-824.
21 J. Wang, C. Yan, K. J. Chee and P. S. Lee, *Adv. Mater.*, 2015, **27**, 2876-2882.
22 M. Giovanni and M. Pumera, *Electroanal.*, 2012, **24**, 615-617.
23 W. Liu, C. Lu, X. Wang, R. Y. Tay and B. K. Tay, *ACS Nano*, 2015, **9**, 1528-1542.
24 S. Wu, K. S. Hui and K. N. Hui, *J. Phys. Chem. C*, 2015, **119**, 23358-23365.
25 Z. Qiao, X. Yang, S. Yang, L. Zhang and B. Cao, *Chem. Comm.*, 2016, **52**, 7998-8001.
26 Z. Yu, C. Li, D. Abbitt and J. Thomas, *J. Mater. Chem. A*, 2014, **2**, 10923-10929.
27 R. Yuksel, S. Coskun and H. E. Unalan, *Electrochim. Acta*, 2016, **193**, 39-44.
28 C. Yan, X. Wang, M. Cui, J. Wang, W. Kang, C. Y. Foo and P. S. Lee, *Adv. Energ. Mater.*, 2014, **4**, 1301396.

Nanoscale Horizons Accepted Manuscript

Please do not adjust margins

View Article Online
DOI: 10.1039/C7NH00024C

29 S. Ye, A. R. Rathmell, Z. Chen, I. E. Stewart and B. J. Wiley, *Adv. Mater.*, 2014, **26**, 6670-6687.
30 Y. Sun, Z. Tao, J. Chen, T. Herricks and Y. Xia, *J. Am. Chem. Soc.*, 2004, **126**, 5940-5941.
31 L. Hu, H. S. Kim, J.-Y. Lee, P. Peumans and Y. Cui, *ACS Nano*, 2010, **4**, 2955-2963.
32 H. Lee, S. Hong, J. Lee, Y. D. Suh, J. Kwon, H. Moon, H. Kim, J. Yeo and S. H. Ko, *ACS Appl. Mater. Interfaces*, 2016, **8**, 15449-15458.
33 A. R. Rathmell, M. Nguyen, M. Chi and B. J. Wiley, *Nano Lett*, 2012, **12**, 3193-3199.
34 H. Eom, J. Lee, A. Pichitpajongkit, M. Amjadi, J. H. Jeong, E. Lee, J. Y. Lee and I. Park, *Small*, 2014, **10**, 4171-4181.
35 D. G. Lee, D. Lee, J. S. Yoo, S. Lee and H. S. Jung, *Nano Convergence*, 2016, **3**, 20.
36 X. Yan, J. Ma, H. Xu, C. Wang and Y. Liu, *J. Phys. D Appl. Phys.*, 2016, **49**, 325103.
37 A. Y. Kim, M. K. Kim, C. Hudaya, J. H. Park, D. Byun, J. C. Lim and J. K. Lee, *Nanoscale*, 2016, **8**, 3307-3313.
38 H. Y. Jung, M. B. Karimi, M. G. Hahm, P. M. Ajayan and Y. J. Jung, *Sci. Rep.*, 2012, **2**, 773.
39 N. Li, G. Yang, Y. Sun, H. Song, H. Cui, G. Yang and C. Wang, *Nano Lett.*, 2015, **15**, 3195-3203.
40 W. Hu, X. Niu, L. Li, S. Yun, Z. Yu and Q. Pei, *Nanotechnology*, 2012, **23**, 344002.
41 T. W. Lin, C. S. Dai and K. C. Hung, *Sci. Rep.*, 2014, **4**, 7274.
42 M. Jamal, M. Hasan, M. Schmidt, N. Petkov, A. Mathewson and K. M. Razeeb, *J. Electrochem. Soc.*, 2013, **160**, B207-B212.
43 Y.-J. Song, J. Chen, J.-Y. Wu and T. Zhang, *J. Nanomater.*, 2014, **2014**, 1-7.
44 S. Gong, Y. Zhao, Q. Shi, Y. Wang, L. W. Yap and W. Cheng, *Electroanal.*, 2016, **28**, 1298-1304.
45 L. Basirico and G. Lanzara, *Nanotechnology*, 2012, **23**, 305401.
46 X. Chen, H. Lin, P. Chen, G. Guan, J. Deng and H. Peng, *Adv. Mater.*, 2014, **26**, 4444-4449.
47 C.-Y. Kao and K.-S. Chou, *J. Power Sources*, 2010, **195**, 2399-2404.
48 C. Zhou, Y. Zhang, Y. Li and J. Liu, *Nano Lett.*, 2013, **13**, 2078-2085.

Published on 19 April 2017. Downloaded on 20/04/2017 08:52:05.

Nanoscale Horizons Accepted Manuscript

This journal is © The Royal Society of Chemistry 20xx